GEORGE BROWN PRESS
JOURNALS, BOOKS & PROCEEDINGS

International Journal of Engineering Advances

Article

Effect of Air Gap Eccentricity on the Torque and Losses of Bulb Tubular Turbine Generators

Shuai Wang [1,*]

[1] College of Electrical and Information Engineering, Lanzhou University of Technology, Lanzhou, China
* Correspondence: Shuai Wang, College of Electrical and Information Engineering, Lanzhou University of Technology, Lanzhou, China

Abstract: The uniformity of the air gap is crucial to the electromagnetic performance of the Bulb Tubular Turbine Generator (BTTG). However, due to factors such as manufacturing tolerances, assembly deviations, and mechanical deformations during operation, the center of the air gap may shift relative to the rotor axis. This air gap eccentricity causes unevenness in the air gap between the stator and rotor along the circumferential direction, leading to a distortion of the magnetic flux density. As a result, the generator's operational stability is compromised, and the fatigue loss of the core material is accelerated. Therefore, the study of the impact of air gap eccentricity on the BTTG is of significant engineering importance for optimizing the generator's structural design and enhancing its operational performance.

Keywords: Bulb Tubular Turbine Generator; air gap eccentricity; torque pulsation; eddy current loss

1. Introduction

Air gap eccentricity is one of the most widely studied issues in the research of generator electromagnetic characteristics, typically classified into static eccentricity, dynamic eccentricity, and mixed eccentricity. Static eccentricity refers to the condition where the rotor center is offset from the stator center but remains unchanged over time, while dynamic eccentricity is characterized by the rotor rotating along an eccentric trajectory, different from the stator center. Mixed eccentricity is the combination of both static and dynamic eccentricity. Studies have shown that air gap eccentricity not only leads to magnetic field distortion, but also causes electromagnetic force imbalance, torque pulsation, and increased losses, thereby affecting the generator's performance.

Bai et al. analyzed the temperature field distribution before and after the air gap eccentricity in the generator. The research indicated that air gap eccentricity increases the iron losses in the windings, leading to a rise in stator winding temperature [1]. Tao et al. through the establishment of a 3D finite element model of the generator, simulated the temperature field of the stator core under static air gap eccentricity conditions [2]. The study found that an increase in air gap eccentricity significantly increases the hysteresis loss and eddy current loss in the stator core, resulting in a rise in temperature. Additionally, through finite element calculations and experimental research, further discovered that the temperature rise caused by eccentricity increases significantly with load, and the highest temperature regions typically occur on the side near the smaller air gap [3].

Air gap eccentricity also leads to additional electromagnetic torque harmonics, affecting the stability of the motor. Inclined eccentricity induces a second harmonic component in the electromagnetic torque [4]. As the eccentricity angle increases, the DC component and second harmonic component in the electromagnetic torque also increase. Wang et al. analyzed the effect of air gap eccentricity on the air gap magnetic field of synchronous motors under both no-load and load conditions using the magnetic circuit method

Received: 12 March 2025
Revised: 18 March 2025
Accepted: 27 March 2025
Published: 31 March 2025

and Maxwell tensor method [5]. By combining total harmonic distortion (THD), electromagnetic torque, and torque fluctuation, structural optimization was performed, yielding optimized design parameters that effectively reduced the negative impact of eccentricity on electromagnetic performance. Furthermore, the electromagnetic characteristics of the generator under conditions of axial and radial static eccentricity [6]. The analysis showed that radial eccentricity primarily increases the DC component, second harmonic, and fourth harmonic components, while axial eccentricity reduces certain harmonic components, revealing different effects of eccentricity on electromagnetic characteristics.

Air gap eccentricity can also induce unbalanced magnetic pull, which in turn triggers vibration issues in the generator unit. The unbalanced magnetic pull under different eccentricity conditions in megawatt-level high-speed permanent magnet synchronous motors, and further explored its impact on vibration characteristics [7]. Similarly, the effect of inclined eccentricity on rotor vibration in synchronous generators, finding that the magnetic pull caused by eccentricity is unevenly distributed along the axial direction, with larger magnetic pull at smaller air gaps [8]. The second harmonic predominantly drives rotor vibration. Zhu et al. conducted a comparative study using numerical analysis and finite element calculation methods to examine the rotor unbalanced magnetic pull under three different air gap eccentricity faults in synchronous motors, providing an important theoretical basis for the study of air gap eccentricity faults in motors [9]. In practical applications, air gap eccentricity often interacts with other faults, generating more complex electromagnetic disturbances. Shaft voltage characteristic analysis was used to reveal the effects of air gap eccentricity and winding inter-turn short circuits on the shaft voltage spectrum of generators [10]. The study found that static eccentricity primarily causes changes in odd harmonics, while winding short circuits mainly affect fractional or even-order harmonics, offering a theoretical basis for online monitoring of hydroelectric generators.

This paper primarily investigates the impact of air gap eccentricity on the generator's air gap magnetic field, electromagnetic force distribution, torque, and loss characteristics. It reveals the relationship between static eccentricity, dynamic eccentricity, and mixed eccentricity with changes in electromagnetic performance. The study systematically uncovers the effects of air gap eccentricity on the operational characteristics of the Bulb Tubular Turbine Generator (BTTG), providing theoretical support and engineering references for improving the generator's air gap distribution and reducing electromagnetic vibration and losses.

2. Model Establishment and Verification

2.1. Establishment of the Generator Electromagnetic Field Model

This paper takes the Bulb Tubular Turbine Generator (BTTG) model SFWG24-88/7820 as the research object, with the basic parameters of the generator shown in Table 1. The stator windings of the Bulb Tubular Turbine Generator are typically designed with a fractional-slot configuration and a relatively high pole pair number. When studying periodic distribution issues (such as electromagnetic performance under steady-state operating conditions), due to the periodic nature of the generator structure, it is divided into 22 computational units, and only one unit is solved to reduce computational complexity and improve efficiency. A contour diagram of the generator's two-dimensional cross-section is shown in Figure 1.

Table 1. Basic Parameters for Electromagnetic Modeling of the Generator.

Parameter	Value	Parameter	Value
Rated Power (kW)	24,000	Stator Inner Diameter (mm)	7370
Rated Voltage (kV)	10.5	Air Gap Length (mm)	10
Rated Current (A)	1389	Number of Poles	88
Rated Speed (rpm)	68.18	Number of Parallel Branches	1
Stator Outer Diameter (mm)	7820	Winding Connection Type	Y

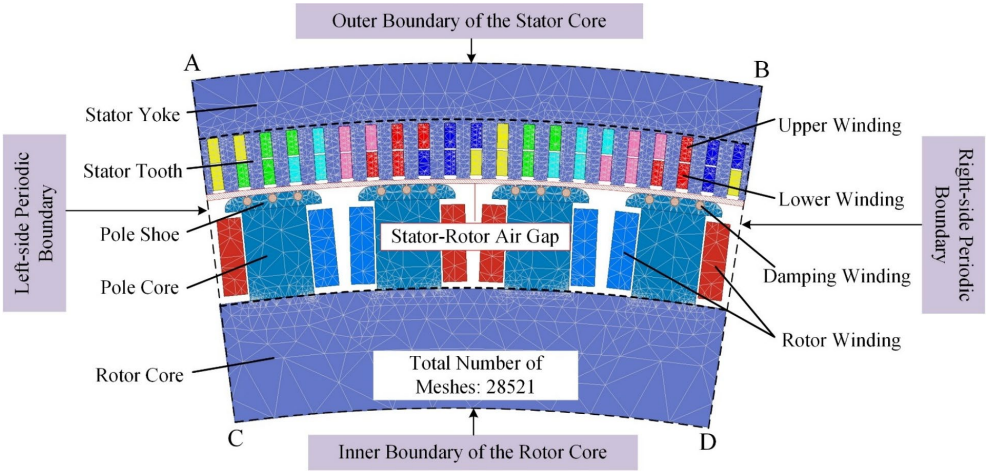

Figure 1. Schematic Diagram of the Unit Generator Structure and Solution Domain.

To simplify the analysis and calculation, the following assumptions are made [11,12]:

1) No leakage flux on the stator core outer side and rotor core inner side;
2) Displacement current is neglected, and the electromagnetic field is considered quasi-static;
3) The core material has uniform magnetic permeability, and the shaft is non-magnetic;

Leakage inductance and reactance at the ends of stator and damping windings are neglected.

However, for non-periodic distribution problems (such as air gap eccentricity), the magnetic field characteristics no longer exhibit a periodic distribution along the circumference of the machine. Therefore, in such operating conditions, a full machine model must be established to ensure the accuracy and applicability of the computational results. In the full machine model, there are no periodic boundary conditions, and only the Dirichlet boundary condition for the axial component of the magnetic vector potential A_Z needs to be specified. The boundary value problem equation system for the two-dimensional nonlinear time-varying electromagnetic field of the full machine model is given by Equation (1):

$$\begin{cases} A_Z|_{Stator\_outer} = 0 \\ A_Z|_{Rotor\_inner} = 0 \\ \frac{\partial}{\partial x}\left(v \cdot \frac{\partial A_Z}{\partial x}\right) + \frac{\partial}{\partial y}\left(v \cdot \frac{\partial A_Z}{\partial y}\right) = -J_{SZ} + \sigma \frac{\partial A_Z}{\partial t} + \sigma v_x \frac{\partial A_Z}{\partial x} \end{cases} \quad (1)$$

Where A_Z is the z-axis component of the magnetic vector potential; J_{SZ} is the z-axis component of the source current density provided by the stator and rotor windings; v is the magnetic reluctivity; and σ is the electrical conductivity of the medium.

2.2. Verification of the Generator Electromagnetic Field Model

Based on finite element simulation data and experimental data, the no-load operating characteristic curve and rated load characteristic curve can be obtained, as shown in Fig-

ure 2. In the figure, the horizontal axis represents the rotor excitation current, the left vertical axis represents the induced voltage, and the right vertical axis represents the armature current. By comparing the no-load induced voltage at different excitation currents with the armature current under rated load conditions, it is found that the error between the two is controlled within 7%. This indicates that the established electromagnetic field model can accurately reflect the operating characteristics of the generator, meeting the requirements of engineering research and providing a foundation for the subsequent analysis in this paper.

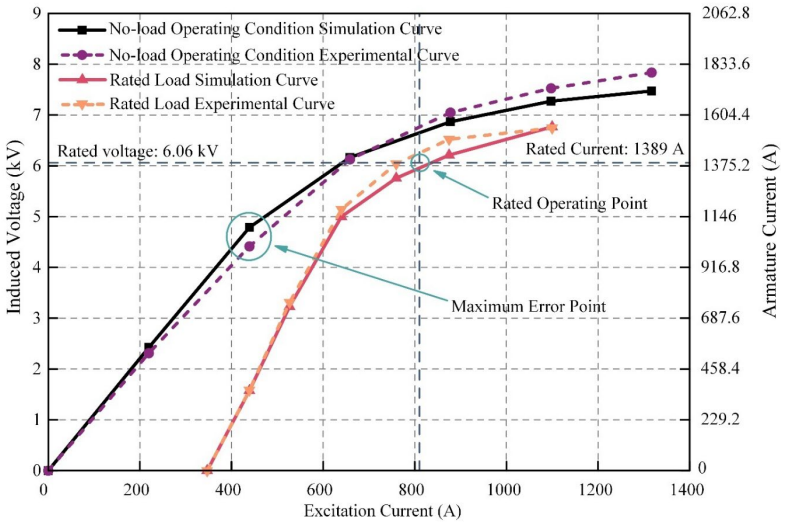

Figure 2. Comparison of Finite Element Calculation Results and Experimental Data.

3. Air Gap Magnetic Flux Density Analysis

3.1. Air Gap Eccentricity Structural Information

As shown in Figure 3, the schematic diagram of the air gap eccentricity structure, static eccentricity refers to the condition where the rotor center is displaced from the stator center but continues to rotate around its own axis. In this state, the air gap distribution varies with spatial position, but the location of the minimum air gap remains fixed, and the air gap size does not change over time.

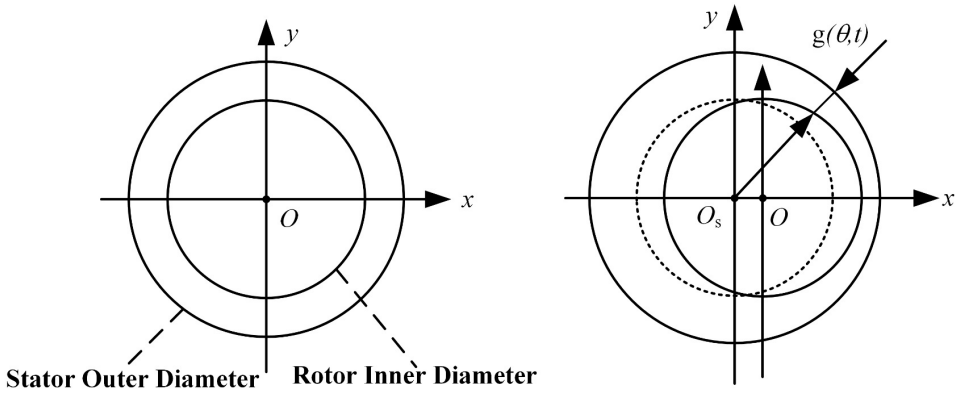

(a) Non-eccentric State (b) Eccentric State.

Figure 3. Schematic Diagram of Air Gap Eccentricity Structure.

Its air gap distribution can be expressed as:

$$g(\theta) = g_0 + e_s \cos\theta \quad (2)$$

Dynamic eccentricity refers to the condition where the rotor center rotates around the stator center, while the rotor's geometric center does not strictly maintain alignment with the stator center. In this case, the location of the minimum air gap changes as the rotor rotates, causing the air gap size to vary not only with spatial position but also to change periodically with time. Its air gap distribution can be expressed as:

$$g(\theta) = g_0 + e_d \cos(\theta - \omega t) \quad (3)$$

Mixed eccentricity is the combination of static and dynamic eccentricities. The air gap variation simultaneously exhibits characteristics of both, meaning it is influenced by the rotor's spatial offset and undergoes dynamic changes over time, resulting in a more complex magnetic field distribution:

$$g(\theta, t) = g_0 + e_s \cos(\theta) + e_d \cos\theta - \omega t \quad (4)$$

Where g_0 is the initial air gap value in the non-eccentric state, e_s is the static eccentricity amount, e_d is the dynamic eccentricity amount, θ is the angular position, and ω is the rotor angular velocity.

3.2. Radial and Tangential Air Gap Magnetic Flux Density Analysis

The distribution of the air-gap magnetic field directly affects the electromagnetic performance of the generator, and eccentricity can lead to uneven magnetic flux density distribution, thereby impacting the operational stability of the generator. The analysis of static eccentricity not only effectively reveals the variation in the air-gap magnetic flux density but also indirectly reflects the influence of dynamic and mixed eccentricity on the air-gap magnetic flux density. Therefore, to simplify the analysis, the variations in radial and tangential air-gap magnetic flux density under different static eccentricities are analyzed, with their variation curves shown in Figures 4.

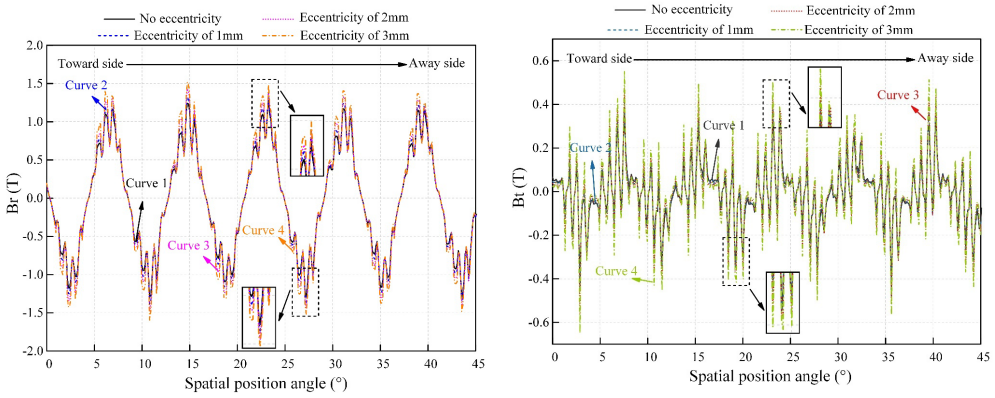

(a) Radial air-gap magnetic flux density (b) Tangential air-gap magnetic flux density

Figure 4. Air-gap magnetic flux density curve under static eccentricity.

As shown in Figure 4(a), when there is no eccentricity, the radial magnetic flux density curve is relatively smooth, with the flux density evenly distributed in space. As the eccentricity increases, the amplitude of fluctuations in the flux density curve gradually increases, with a significant rise in the flux density on the Toward side and a corresponding decrease on the Away side, indicating that the radial air-gap magnetic flux density distribution undergoes a noticeable change due to the eccentricity. From Figure 4(b), it can be observed that the variation trend of the tangential magnetic flux density curve is similar to that of the radial magnetic flux density. As eccentricity increases, the flux density on the Toward side rises, and the flux density on the Away side decreases. However, compared to the radial magnetic flux density, the fluctuation frequency of the tangential magnetic flux density curve is higher.

4. Electromagnetic Force Analysis under Eccentricity

In the study of electromagnetic forces in turbine generators, the distribution of the magnetic field in the air gap is a key factor affecting the calculation of electromagnetic force density. To accurately describe the magnetic field in the air gap, Fourier series can be used to represent the flux density as a sum of different harmonic components. This allows for an effective analysis of the magnetic field distribution in the air gap and its variation over time and space. The expression for the air gap flux density is given by equation (5):

$$\begin{cases} B_r(\theta,t) = \sum_{k=1}^{n} B_{rk}\cos[k\alpha - \theta_{rk}(t)] \\ B_t(\theta,t) = \sum_{k=1}^{n} B_{tk}\cos[k\alpha - \theta_{tk}(t)] \end{cases} \tag{5}$$

In the equation, $B_r(\theta,t)$ and $B_t(\theta,t)$ represent the radial and tangential components of the air gap flux density, respectively; B_{rk} and B_{tk} represent the amplitudes of the radial and tangential flux densities; θ_{rk} and θ_{tk} represent the phases of the radial and tangential flux densities.

Based on the air gap flux density, the tangential electromagnetic force density can be further calculated using the Maxwell stress tensor method. The calculation formula is given by equation (6):

$$F_t(\theta,t) = \frac{1}{\mu_0}[B_r(\theta,t)B_t(\theta,t)] \tag{6}$$

In the equation, $F_t(\theta,t)$ represents the tangential electromagnetic force density in the air gap, in N/m²; μ_0 represents the magnetic permeability of air.

As shown in Figure 5, under the condition of no eccentricity, the tangential electromagnetic force density distribution is uniform, with a smooth waveform and small variation amplitude. As the static eccentricity increases, the electromagnetic force waveform gradually becomes more complex and irregular. When the static eccentricity reaches 1mm, disturbances begin to appear in the electromagnetic force density. At eccentricities of 2mm and 3mm, the waveform fluctuates violently, the differences increase, and the waveform becomes more irregular. Numerically, as the eccentricity increases, the maximum value rises from 4×10^5 N/m² to 5.97×10^5 N/m², and the minimum value drops from -1.3×10^5 N/m² to -2.66×10^5 N/m². Although the difference between the maximum and minimum values increases, the average value remains at 3.37×10^4 N/m², indicating that the overall electromagnetic force density changes little, but the fluctuations are significantly enhanced.

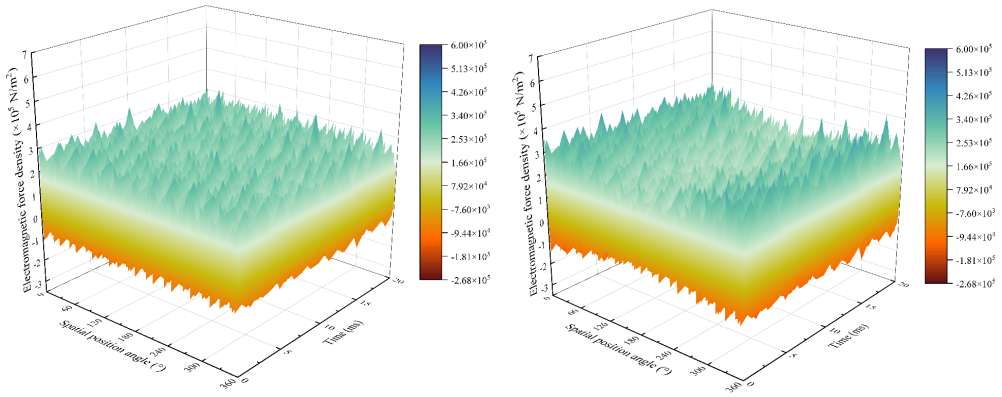

(a) No Eccentricity Condition (b) Eccentricity of 1 mm

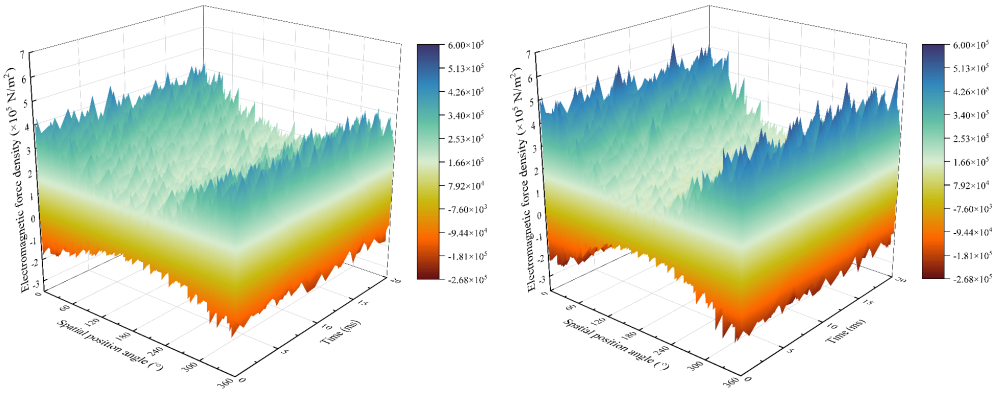

(c) Eccentricity of 2 mm (d) Eccentricity of 3 mm

Figure 5. Tangential Electromagnetic Force Density under Different Static Eccentricities.

In the case of static eccentricity, the peaks are fixed on the displaced side, whereas dynamic eccentricity causes the peaks and valleys to vary with time and angle. To further study the impact of electromagnetic force variations under different eccentricity conditions on the generator's performance, the next step will analyze the effects of air gap eccentricity on average torque and torque pulsation.

5. Torque Characteristics Analysis

Further analysis of the effects of static eccentricity, dynamic eccentricity, and mixed eccentricity on the electromagnetic torque is presented. The variations in average torque and torque pulsation are shown in Figure 6.

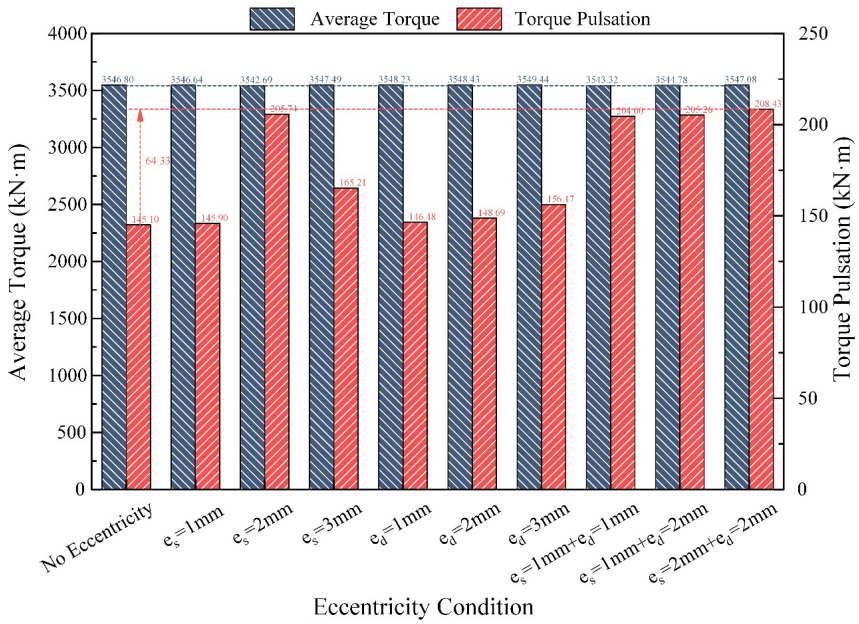

Figure 6. Average Torque and Torque Pulsation under Different Eccentricity Conditions.

As seen in Figure 6, the effect of different eccentricity conditions on the average torque is relatively small, remaining between 3543 kN·m and 3549 kN·m. Further analysis combined with Table 2 reveals that eccentricity has a significant impact on torque pulsation, especially under static and mixed eccentricity conditions, where the increase in torque pulsation is more pronounced.

Table 2. Torque Pulsation Coefficient under Eccentricity.

Eccentricity Condition	K_{TP}
No Eccentricity	0.0409
$e_s = 1mm$	0.0411
$e_s = 2mm$	0.0581
$e_s = 3mm$	0.0466
$e_d = 1mm$	0.0413
$e_d = 2mm$	0.0419
$e_d = 3mm$	0.044
$e_s = 1mm + e_d = 1mm$	0.0577
$e_s = 1mm + e_d = 2mm$	0.0579
$e_s = 2mm + e_d = 2mm$	0.0588

To measure the degree of torque fluctuation in the generator under different air gap lengths, the torque pulsation coefficient K_{TP} is defined as:

$$K_{TP} = \frac{T_{max} - T_{min}}{T_{avg}} \quad (7)$$

Where T_{max} is the maximum torque, T_{min} is the minimum torque, and T_{avg} is the average torque. This coefficient reflects the relative intensity of torque fluctuations during the operation of the generator. A larger value indicates that the impact of torque pulsations relative to the average torque is more significant.

When $e_s = 1mm$, the change in torque pulsation is minimal. However, when $e_s = 2mm$, the torque pulsation increases from $145.1\ \text{kN} \cdot \text{m}$ to $205.74\ \text{kN} \cdot \text{m}$, and the torque pulsation coefficient increases from 0.0409 to 0.0581, indicating a significant enhancement in electromagnetic torque fluctuations. When e_s is further increased to 3mm, the torque pulsation decreases to $165.21\ \text{kN} \cdot \text{m}$, but it remains much higher than under the no-eccentricity condition. In contrast, dynamic eccentricity has a smaller effect on torque pulsation. When e_d increases from 1 mm to 3 mm, the torque pulsation only increases from 146.48 kN·m to 156.17 kN·m, with a gentler variation.

Under mixed eccentricity conditions, the torque pulsation is further amplified. When $e_s = 1mm + e_d = 1mm$, the torque pulsation increases to $204.6\ \text{kN} \cdot \text{m}$, which is significantly higher than in the individual eccentricity conditions. When $e_s = 2mm + e_d = 2mm$, the torque pulsation reaches $208.43\ \text{kN} \cdot \text{m}$, the highest value among all eccentricity conditions, and the torque pulsation coefficient increases to 0.0588. This indicates that the combined effect of static and dynamic eccentricity further amplifies electromagnetic torque fluctuations.

6. Loss Characteristics Analysis

Air gap eccentricity is directly influenced by the uneven magnetic field, primarily affecting the rotor magnetic poles and damping bars. Therefore, further research is conducted to study the impact of air gap eccentricity on the loss characteristics of the rotor magnetic poles and damping bars (Figure 7).

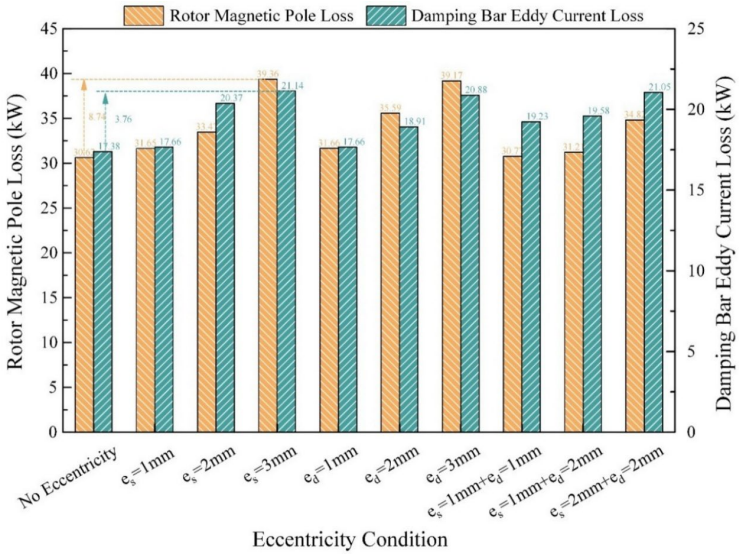

Figure 7. Magnetic Pole Loss and Damping Bar Eddy Current Loss under Eccentricity Conditions.

The rotor magnetic pole loss increases progressively with the increase in eccentricity. In the no-eccentricity condition, the rotor magnetic pole loss is 30.62 kW. As the static eccentricity increases, the rotor magnetic pole loss gradually rises. When $e_s = 3mm$, the loss is 39.36 kW, an increase of 8.74 kW, which is about 1.29 times that of the no-eccentricity condition. In the dynamic eccentricity condition, the variation trend of the rotor magnetic pole loss is similar to that of static eccentricity. When $e_d = 3mm$, the loss is 39.17 kW, an increase of 8.55 kW, approximately 1.28 times the value in the no-eccentricity condition. It can be seen that the increase in eccentricity under different eccentricity conditions gradually exacerbates the impact on the rotor magnetic pole loss.

Under mixed eccentricity conditions, the rotor magnetic pole loss and damping bar eddy current loss exhibit a clear superposition effect. As the eccentricity increases, the rotor magnetic pole loss gradually increases, but the increase is not simply a linear superposition. When $e_s = 1mm + e_d = 1mm$, the rotor magnetic pole loss is 30.77 kW, slightly lower than the 30.62 kW in the no-eccentricity condition, indicating that the two eccentricity effects cancel each other out, resulting in a slight decrease in loss. As the dynamic eccentricity increases to 2mm ($e_s = 1mm + e_d = 2mm$), the loss rises to 31.21 kW, an increase of 0.59 kW. When the eccentricity is further increased ($e_s = 2mm + e_d = 2mm$), the loss significantly increases to 34.82 kW, an increase of 4.2 kW, much higher than in the single eccentricity condition.

The damping bar eddy current loss increases significantly with the increase in eccentricity. In the no-eccentricity condition, the damping bar eddy current loss is 17.38 kW. As the static and dynamic eccentricity increase, the loss gradually rises. When $e_s = 1mm$, the loss is 17.66 kW. When $e_s = 2mm$ and $e_s = 3mm$, the loss increases to 20.37 kW and 21.14 kW, respectively. When $e_d = 1mm$, the loss is 17.66 kW, and when $e_d = 2mm$, the loss is 20.88 kW, with similar increases.

Similarly, under mixed eccentricity conditions, the damping bar eddy current loss shows a similar growth trend. When $e_s = 1mm + e_d = 1mm$, the loss is 19.23 kW, noticeably higher than in the individual static and dynamic eccentricity conditions, indicating that when static and dynamic eccentricities are combined, the superimposed eccentricity effect significantly increases the damping bar eddy current loss. As the eccentricity increases further, when $e_s = 2mm + e_d = 2mm$, the loss reaches 21.05 kW, reflecting the superimposed effect of the magnetic field inhomogeneity on the eddy current loss under mixed eccentricity conditions.

The rotor magnetic pole loss in the hydraulic turbine generator is mainly concentrated at the pole shoes. As shown in Figure 8, the rotor magnetic pole hysteresis loss

shows minimal variation and has a low amplitude. Therefore, the primary focus is on analyzing the impact of air gap eccentricity on the eddy current loss at the pole shoes.

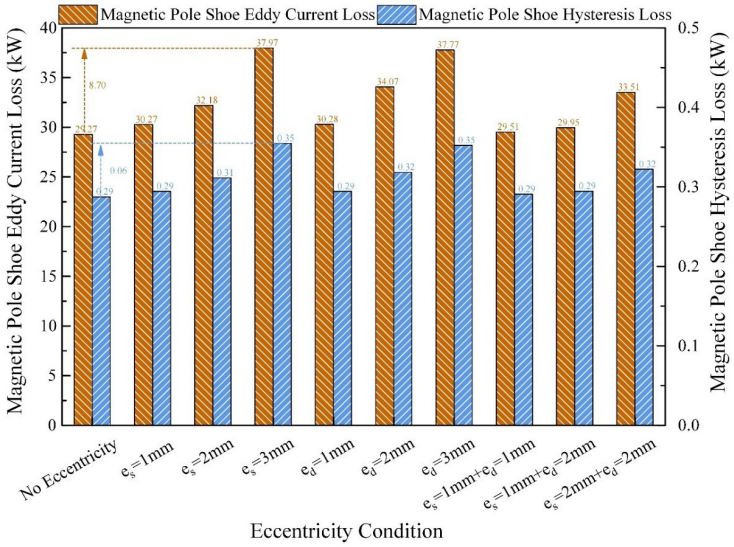

Figure 8. Magnetic Pole Shoe Loss under Eccentricity Conditions.

As shown in Figure 8, the eddy current loss in the pole shoes increases significantly with the increase in eccentricity. In the no-eccentricity condition, the eddy current loss is 29.27 kW. When $e_s = 1mm$, the eddy current loss increases to 30.27 kW, an increase of approximately 3.4%. When $e_s = 3mm$, the eddy current loss further increases to 37.97 kW, an increase of 29.7%.

In the dynamic eccentricity condition, the variation trend of the eddy current loss is similar to that of static eccentricity. When $e_d = 3mm$, the eddy current loss is 37.77 kW, which is close to the 37.97 kW at $e_s = 3mm$, indicating that the effect of dynamic eccentricity on eddy current loss is comparable to static eccentricity, with only a small difference between the two.

Under mixed eccentricity conditions, the eddy current loss also shows a clear growth trend, exhibiting a superposition effect. When $e_s = 1mm + e_d = 1mm$, the eddy current loss is 29.51 kW, slightly higher than in the no-eccentricity condition. As the static and dynamic eccentricity increase, the eddy current loss continues to rise. When $e_s = 2mm + e_d = 2mm$, the eddy current loss reaches 33.51 kW, an increase of 14.5% compared to the no-eccentricity condition, further validating the superposition effect of magnetic field inhomogeneity under mixed eccentricity.

7. Conclusion

This paper investigates the effects of air-gap eccentricity on the performance of bulb tubular hydro-generators, including the distribution of air-gap magnetic flux density, electromagnetic force density, torque ripple, as well as pole and damper bar losses. The specific conclusions are as follows:

1) From the perspective of air-gap magnetic flux density distribution, both the radial and tangential flux density curves are relatively smooth and evenly distributed when there is no eccentricity. As the eccentricity increases, the flux density on the Toward side rises, while that on the Away side decreases. Moreover, the fluctuation frequency of the tangential flux density is higher than that of the radial flux density, indicating that eccentricity enhances the non-uniformity of the air-gap magnetic field distribution.
2) In the absence of eccentricity, the tangential electromagnetic force density exhibits a uniform distribution with a smooth waveform and small variations. As the

eccentricity increases, the amplitude difference in electromagnetic force density between the Toward side and the Away side gradually increases, while the mean value of the electromagnetic force density remains relatively unchanged. This indicates that eccentricity has little effect on the overall electromagnetic force density but mainly enhances its fluctuation and intensifies local differences.

3) In terms of torque characteristics, eccentricity has a minor effect on the average torque of the generator but significantly impacts torque pulsation. When static eccentricity increases from 1mm to 2mm, the torque pulsation coefficient rises from 0.0409 to 0.0581, indicating a significant increase in the fluctuation of the electromagnetic torque. In contrast, dynamic eccentricity has a relatively smaller impact on torque pulsation. Under mixed eccentricity conditions, the torque pulsation further increases, suggesting that the combined effect of static and dynamic eccentricity amplifies the electromagnetic torque pulsation.
4) As the air gap eccentricity increases, both rotor magnetic pole loss and damping bar eddy current loss show an upward trend. Under mixed eccentricity conditions, as static and dynamic eccentricities increase, the superimposed effect is significantly enhanced. Additionally, the hysteresis loss at the rotor magnetic pole shoes shows small amplitude and minimal variation, indicating that air gap eccentricity primarily affects rotor losses by enhancing the eddy current effects at the pole shoes.

Conflicts of Interest: The authors declare that they have no conflict of interest.

References

1. Y.-L. He et al., "Impact of 3D air gap eccentricity on winding insulation temperature characteristic in PMSG," *Alexandria Eng. J.*, vol. 93, pp. 220-235, 2024, doi: 10.1016/j.aej.2024.03.015.
2. W. Tao, Y. He, H. Lei, et al., "Research on stator-core temperature characteristics under static air-gap eccentricity in turbo-generator," in *Proc. 2020 IEEE Int. Conf. Artif. Intell. Inf. Syst. (ICAIIS)*, IEEE, 2020, pp. 637-642, doi: 10.1109/ICAIIS49377.2020.9194940.
3. Y. -L. He et al., "Impact of Static Air-Gap Eccentricity on Thermal Responses of Stator Winding Insulation in Synchronous Generators," in *IEEE Trans. Ind. Electron.*, vol. 69, no. 12, pp. 13544-13554, Dec. 2022, doi: 10.1109/TIE.2021.3135627.
4. Y. He, Z. Fu, D. Dai, et al., "Effect of axial air gap asymmetric faults on the electromagnetic torque characteristics of generators," *J. Hebei Univ. (Nat. Sci. Ed.)*, vol. 45, no. 01, pp. 1-9, 2025, doi: 10.3969/j.issn.1000-1565.2025.01.001.
5. J. Wang and Y. Wang, "Electromagnetic torque analysis and structure optimization of interior permanent magnet synchronous machine with Air-Gap eccentricity," *Energies*, vol. 16, no. 4, p. 1665, 2023, doi: 10.3390/en16041665.
6. A. Laiho, A. Sinervo, J. Orivuori, K. Tammi, A. Arkkio and K. Zenger, "Attenuation of Harmonic Rotor Vibration in a Cage Rotor Induction Machine by a Self-Bearing Force Actuator," in *IEEE Transactions on Magnetics*, vol. 45, no. 12, pp. 5388-5398, Dec. 2009, doi: 10.1109/TMAG.2009.2026168.
7. O. N. Molokanov, "A comparative analysis of rolling-rotor electrical machines of different winding designs," *Russian Elect. Eng.*, vol. 95, no. 6, pp. 486-492, 2024, doi: 10.3103/S1068371224700536.
8. Y. -L. He et al., "Impact of Stator Interturn Short Circuit Position on End Winding Vibration in Synchronous Generators," in *IEEE Transactions on Energy Conversion*, vol. 36, no. 2, pp. 713-724, June 2021, doi: 10.1109/TEC.2020.3021901.
9. R. Zhu, X. Tong, Q. Han, et al., "Calculation and analysis of unbalanced magnetic pull of rotor under motor air gap eccentricity fault," *Sustainability*, vol. 15, no. 11, p. 8537, 2023, doi: 10.3390/su15118537.
10. I. Zaitsev, A. Levytskyi, and V. Bereznychenko, "Hybrid diagnostics systems for power generators faults: systems design principle and shaft run-out sensors," in *Power Systems Research and Operation*, O. Kyrylenko, A. Zharkin, O. Butkevych, I. Blinov, I. Zaitsev, and A. Zaporozhets, Eds. Cham, Switzerland: Springer, 2022, vol. 388, pp. 71-98. ISBN: 9783030829254.
11. H. Qiu and X. Fan, "The influence of asymmetric pole shoe on synchronous hydro generator," *IEEJ Trans. Electr. Electron. Eng.*, vol. 13, no. 11, pp. 1654-1659, 2018, doi: 10.1002/tee.22728.
12. H. Qiu, X. Fan, R. Yi, et al., "Eddy current density asymmetric distribution of damper bars in bulb tubular turbine generator," *Arch. Electr. Eng.*, vol. 66, no. 3, pp. 571-581, 2017, doi: 10.1515/aee-2017-0043.